Modeling and Control System Design of a Crystallizer Train for Para-xylene Production

Souichi Amano * **Genichi Emoto** * **Hiroya Seki** **

* *Production Technology Department, Mitsubishi Chemical Corporation, Kurashiki, 712-8054 Japan*
** *Chemical Resources Laboratory, Tokyo Institute of Technology, Yokohama, 226-8503 Japan*
(Corresponding author, e-mail: hseki@ pse.res.titech.ac.jp)

Abstract: A dynamic process model of an industrial crystallizer train for para-xylene production, which consists of five scraped surface crystallizers, two hydrocyclone separators, and two centrifugal separators, is developed for control system design. The model is identified by using real plant data. Optimal operating policies, which consider feed maximization and load distribution among the crystallizers, are derived, and multiloop controller is configured to realize the operating policy.

Keywords: Crystallization, industrial application, plantwide control

1. INTRODUCTION

Crystallization is one of the most popular unit operations for separation and purification used in the chemical industry. Despite their importance, process and control system design for separation processes based on crystallization technology has received much less attention compared with distillation column processes [Mendez et al. (2005)].

Most of the studies on control system design for crystallization processes focus on operations of a single crystallizer as an isolated unit [Rawlings et al. (1993), Hasebe et al. (2000)], although crystallizers never exist in isolation and simultaneous consideration of subprocessing units such as filtration and drying, etc. should be equally important [Chang et al. (1998)]. Some studies handle operations of multiple crystallizers [Garside (1985), Liu et al. (1991)], but study on process and control system design for crystallization processes from the plantwide perspective is quite limited [Wibowo et al. (2001), Ward et al. (2007)].

In this paper, modeling and control system design of an industrial crystallizer train, which comprises five crystallizers, two centrifugal separators and two cyclone separators, are discussed. The process concerns the product recovery section in a para-xylene production plant. The process underwent several revamps during the course of a long history of commercial operation, and the process became rather complicated, so that quantitative analysis based on a mathematical model would help provide us with improved operations.

First, a dynamic process model is developed, which describes crystallization kinetics, mass balance, and heat balance for the whole plant. The model is then identified by using the actual plant data. Based on the developed model, optimal operating policies are derived through optimization calculations. In setting up the optimization problem, practical considerations such as constraint handling issues are discussed in detail. Finally, a multi-loop control system is configured which realizes the optimal operation.

2. PROCESS DESCRIPTION

2.1 Para-xylene production process

Para-xylene is an aromatic hydrocarbon used primarily to make intermediates for manufacturing polyester. It is the main feedstock for purified terephthalic acid and dimethyl terephthalate, which in turn are used to produce polyethylene terephthalate (PET) for use in fibres for textiles, bottles for soft drinks and water.

Figure 1 shows a typical commercial production process of para-xylene, where fresh feed that contains mixed xylene (mixture of ortho-xylene, meta-xylene, and para-xylene) and ethylebenzene is sent from the upstream plant and pure para-xylene (normally $> 99.5\%$) is recovered from the feedstock by fractionation and crystallization. Crystallization is one of the conventional methods for the recovery of pure para-xylene; currently adsorption may be the most popular. Filtrate from the para-xylene recovery section is sent to the reaction section, where ortho-xylene, meta-

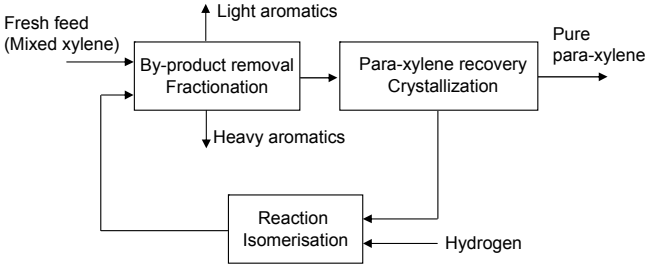

Fig. 1. Typical para-xylene production process

xylene are converted into para-xylene through isomerization reaction.

2.2 Para-Xylene recovery based on crystallization technology

Since many physical properties of the individual xylene isomers are similiar, high purity separation of each individual xylene isomer is difficult. Crystallization is one of the methods for that purpose, resorting to the differences in the melting points among the xylene isomers.

Figure 2 shows the crystallizer train under study, which consists of two separate cyrstallization stages. The first stage uses several (in this example, three) scraped surface crystallizers to bring the temperature of the xylene mixture close to the para-xylene/meta-xylene eutectic point. The first-stage crystallizers are followed by a solid-liquid separation process using a centrifuge (screen-bowl type in this example). The cold xylene filtrate from the first stage cools the feedstream (not shown in the figure) and is sent to the isomerization section. To achieve the maximum production rate from a certain feedstock, the first-stage crystallization temperature should be decreased as low as possible, down to the eutectic point of para-xylene and meta-xylene.

The solid cake para-xylene crystals and the adherent mother liquor from the first stage are melted in the melt tank, and pumped to the second-stage crystallizers. The second stage is made up of the main crystallizer, and the auxiliary crystallizer located on the recycle stream. The slurry from the main crystallizer is sent to the final centrifugal separator, and the filter cake is melted to form the final para-xylene product. A major portion of the mother liqour from the main crystallizer is returned to the first-stage after a part of para-xylene in the mother liquor is recovered by the auxiliary crystallizer.

Due to the presence of the recycle streams at several locations, which have been added during the course of a long history of commercial operation, the process becomes highly interacting, so that careful analysis on the basis of a mathematical model would be necessary in designing control system.

3. MODELING

3.1 Crystallizer

The crystallizers are assumed to be mixed-suspension mixed-product removal (MSMPR) systems. In addition, the following assumptions are made for model development:

- Only growth and nucleation are considered as crystallization kinetics; breakage and agglomeration are ignored.
- Para-xylene crystal growth is fast enough so that the liquid phase para-xylene is always saturated (the assumption of the high growth rate limit). Nucleation occurs at the crystallizer wall.

These assumptions are adopted from the study by Patience et al. (2001), who studied experimentally the crystallization kinetics of para-xylene in a scraped surface crystallizer.

Denoting the crystal size distribution (CSD) in the crystallizer as $f(x,t)$, its $i-$th moment μ_i is defined as

$$\mu_i = \int_0^\infty f(x,t)x^i dx.$$

By using the method of moment, the population balance equation can be written as:

$$\frac{d\mu_0}{dt} = B + \mu_0^{in} - \mu_0^{out},$$
$$\frac{d\mu_i}{dt} = iG\mu_{i-1} + \mu_i^{in} - \mu_i^{out} \qquad (i \geq 1),$$

where B and G are the nucleation rate and growth rate of para-xylene crystal respectively, μ_i^{in} and μ_i^{out} are the moment flows in and out of the crystallizers which can be calculated from the MSMPR assumption. The empirical expression is used for the nucleation rate B:

$$B = k_b \Delta C^b,$$

where ΔC is defined as the supersaturation created by the temperature difference between the magma and the crystallizer wall:

$$\Delta C = \frac{C^*(T) - C^*(T_J)}{C^*(T_J)}.$$

Here, T is the temperature of the magma, T_J is the temperature of the crystallizer wall, which is assumed to be equal to the jacket temperature, and $C^*(T)$ is the temperature dependent solubility of para-xylene.

The mass balance of the liquid phase para-xylene is written as

$$\frac{dm_{PX}}{dt} = F^{in}C^{in} - F^{out}C^*(T) - 3\rho k_v G\mu_2,$$

where m_{PX} is the liquid hold up of para-xylene in the crystallizer, F^{in} and F^{out} are the inlet and outlet liquid flow rates respectively, C^{in} is the para-xylene concentration of the inlet flow, ρ is the density of para-xylene crystals, k_v is the shape factor. Note that the liquid concentration of para-xylene in the crystallizer is assumed to be saturated.

The heat balance is written as

$$\frac{dH}{dt} = H^{in} - H^{out} + 3\rho k_v G\mu_2 \Delta H_c - UA(T - T_J),$$

where H is the overall enthalpy of the crystallizer, H^{in} and H^{out} are the enthalpy in and out of the crystallizer respectively, ΔH_c is the heat of crystallization, and UA is the overall heat transfer coefficient. Because of the fouling of the crystallizer wall, the heat transfer coefficient is treated as slowly time-varying.

The assumption of the high growth rate limit, that is, the growth rate of para-xylene crystals is so large that the liquid phase para-xylene concentration is always saturated, renders the model equations a DAE system; the growth rate is not explicitly given in the above equations. But the model equation can be easily converted into the ODE by the procedure shown by Patience et al. (2001).

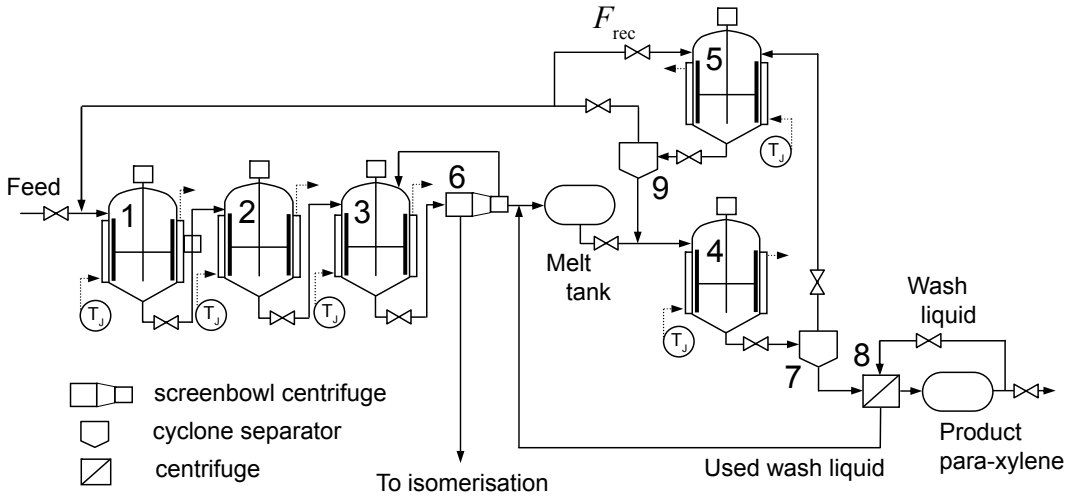

Fig. 2. Process flow of the para-xylene recovery section. The numbers ($1 \sim 9$) denote the equipment numbers which are used as subscript to distiguish the equipments.

3.2 Cyclone separator

The hydrocyclone separates the inlet slurry flow into two streams: the overflow and underflow streams. With the help of centrifugal force, the solid particles contained in the inlet stream are concentrated in the underflow. Ideally the overflow stream contains no solid particle, but it is practically assumed that some of the crystals whose size is smaller than $\bar{d}$ escape into the overflow stream. An ideal separation is assumed, where the crystals over the size $\bar{d}$ will not be included in the overflow. Crystals under the size $\bar{d}$ will be included both in the underflow and overflow, and they are distributed according to the liquid flow rates of these streams.

To obtain the amount of crystals smaller than $\bar{d}$, the crystal size distribution has to be recovered from its associated moment information. However, it is known that infinite number of the moments are needed to reconstruct the CSD [McGraw et al. (1998)].

To avoid this problem, the logarithmic normal distribution is assumed for the CSD. From the values of the moments $\mu_i's$, the mean crystal size m and variance σ^2 can be recovered from the relation:

$$\log(\mu_n/\mu_0) = \frac{n^2}{2}\sigma^2 + nm.$$

In this study, m and σ are determined through the least squares fit by using the moments up to the 4-th order.

Then the amount of crystals below the size $\bar{d}$ can be calculated as

$$\int_0^{\bar{d}} x^n f(x)dx = \exp(\frac{n^2\sigma^2 + 2nm}{2}) \cdot\frac{1}{2}\left(\mathrm{erf}(\frac{\log\bar{d} - m - n\sigma^2}{\sqrt{2}\sigma}) + 1\right),$$

where the error function is defined as

$$\mathrm{erf}(x) = \int_0^x \frac{2}{\pi}\exp(-\lambda^2)d\lambda.$$

No holdup is assumed for the cyclone separators. Then, the balance equations for the hydrocyclone are readily derived.

3.3 Centrifugal separator

At the centrifugal separators, it is assumed that the para-xylene crystals of the size smaller than $\hat{d}$ pass through the screen, accompanying the mother liquor. The amount of such crystals is calculated in the same way as in the hydrocyclone separator model.

Constant void fraction is assumed for the filter cake ($\varepsilon = 0.4$), and the average degree of saturation S_{av} (the percentage of the void in the cake filled with mother liquor) is assumed to be a function of the average crystal size $d_{23} = \mu_3/\mu_2$:

$$S_{av} = S_{av}(\hat{S}, d_{23}),$$

where $\hat{S}$ is a parameter to define the empirical expression.

When the cake is washed (as in the second stage centrifuge), part of the mother liquor in the cake is replaced by the wash liquor. The percentage of the mother liquor replaced by the wash liquid is expressed by the empirical expression, which is a function of S_{av} and the ratio of the amounts of the wash liquid and the mother liqour. The amount of the remaining mother liquor in the cake largely accounts for the product purity.

Then, the balance equations for the centrifuge are readily derived; no holdup is assumed.

The screen-bowl type centrifugal separator at the outlet of the 1st stage is modeled as a combined system comprising a cyclone and a centrifuge; the bowl part is modeled as the cyclone. The parameter α is introduced as the ratio between the bowl filtrate (overflow stream) and the liquid inlet, which will be used for model identification in the next section.

3.4 Overall process model

By combining the models for the crystallizers, the hydrocyclone separators, the centrifugal separators and other

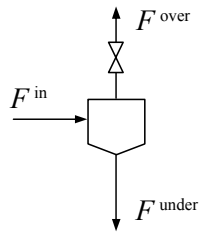

Fig. 3. Hydrocyclone separator modeling

storage tanks, a nonlinear dynamic process model in the following form is derived:

$$\begin{aligned} \dot{x} &= f(x,u,p) \\ y &= h(x,u,p), \end{aligned} \tag{1}$$

where x is the state variable, u is the measured independent variables, p is the unknown parameters and unmeasured independent variables, and y is the measured variables. Here, the variables are defined for the purpose of model identification.

3.5 Model identification

The unknown parameters are obtained through least squares fit of the model calculation with the plant data:

$$\min_{x,p} \quad (\tilde{y}-y)^T(\tilde{y}-y) \tag{2}$$

subject to

$$0 = f(x,u,p), \tag{3}$$

where $\tilde{y}$ is the plant data. Eq. (3) assumes that model identification is done for steady states.

Several data sets for $(\tilde{y},u)$, which have been obtained by heavily filtering 1 hour average data from the real plant, are used for the least squares fit. The available measurements $\tilde{y}$ consist of the holdups of the five crystallizers, the holdups of the melt tank and product tank, the temperatures of the crystallizers, the production rate, the recycle flow rate to the isomerization reaction, paraxylene concentrations of the melt tank and product tank.

As a result of the sensitivity analysis of the minimization problem (2), the identifiable parameter set $p \in \Re^6$ has been selected as

$$p = \left(\alpha_6 \ \bar{d}_6 \ \hat{d}_6 \ \hat{S}_6 \ \hat{S}_8 \ \bar{d}_9\right)^T,$$

where the subscript are defined as equipment number in Fig. 2. The overall heat transfer coefficient UA_i of each crystallizer ($i = 1 \sim 5$) is considered as time-varying and is also used for model identification as the fitting parameters. It should be noted that the parameters concerning crystallization kinetics such as b and k_b are not identifiable from the available measurements, so that their values are adopted from the paper by Patience et al. (2001).

Figure 4 shows one of the fitting results: the parity plot of the fitting result for the production rate. The operation condition used for model identification covers ±20% of the nominal production rate.

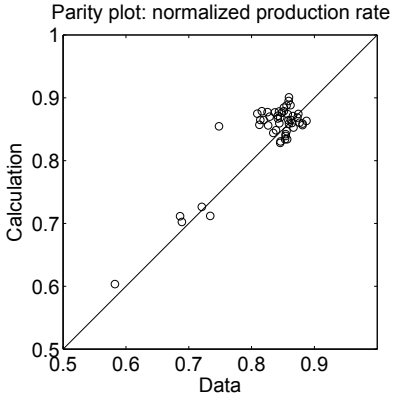

Fig. 4. Parity plot of production rate measurements

4. CONTROL SYSTEM DESIGN

4.1 Definition of manipulated and controlled variables

By using the identified process model, basic regulatory control system is designed; the seven inventory control loops are closed with each effluent flow, and the temperature control loop of each crystallizer is closed by manipulating its corresponding jacket temperature.

The manipulated variables for further control system design are defined as $u_C \in \Re^9$, and they consist of the temperature setpoints of the crystallizers, the ratios of the flow rates of the overflow and the underflow of the cyclones, the wash liquid flow rate, and the recycle flow rate from the overflow of the cyclone to the auxiliary crystallizer:

$$u_C = \left(T_1 \ T_2 \ T_3 \ T_4 \ T_5 \ \alpha_7 \ \alpha_9 \ F_w \ F_{rec}\right)^T,$$

where the subscripts are defined as the equipment number in Fig. 2 and α_i ($i = 7, 9$) is the flow rate ratio in the cyclone separators, and F_w is the wash flow rate, and F_{rec} is the recycle flow rate.

The controlled variables are defined as y_C, for which constraints may be considered, and the process model for control system design is described as

$$\begin{aligned} \dot{x} &= f_C(x,u_C) \\ y_C &= h_C(x,u_C). \end{aligned} \tag{4}$$

4.2 Steady state optimal operation policy

In deriving optimal operating policies, the following constraints are considered.

- *Lower limit for the para-xylene purity x_{prod}* This is a product specification. The purity is determined by the amount of accompanying mother liquor, which is affected by the average crystal size (the larger, the better) and the intensity of the wash at the centrifuge.
- *Lower limits for the jacket temperatures at the 1st stage crystallizers $T_{J,1} \sim T_{J,3}$* The yield of the paraxylene recovery section is determined by how low the 1st stage crystallizer temperature can be reduced. The refrigerator capacity determines the lower limits of the jacket temperatures.
- *Upper limits for the temperature difference between the jacket and crystallizer $\Delta T_1 \sim \Delta T_5$* One of the

major operational concerns is the fouling of the crystallizer wall, which is caused by the crystal deposition on the wall surface and exacerbated by too high a super-saturation at the crystallizer wall. Para-xylene crystal deposition on the wall results in poor heat transfer and limits the production rate.

- *Upper limits for the slurry concentrations in the second stage crystallizers* Cs_4, Cs_5 The slurry concentrations in the second stage crystallizers tend to be high and they are limited by the torque limit of the agitator. If the slurry concentration is too high, mixing in the crystallizer would become imperfect.
- *Upper and lower flow rate limits for the cyclone separators* Operation of the cyclone in an abnormal flow rate regime results in inappropriate classification of crystals.
- *Upper limits for the slurry concentrations in the underflow of the cyclone separators* Cs_7, Cs_9 The slurry concentration in the underflow of the cyclone separator tends to be large. Too high a slurry concentration results in clogging of the pipe.
- *Upper limit for the para-xylene concentration in the melt tank* If this concentration is too high, some of the solid para-xylene with low purity from the 1st stage do not dissolve in the melt tank.

The following two modes of operations are considered for developing optimal operating policies.

Feed maximization Feed maximization is realized by solving the following optimization problem:

$$\max_{u_C} \quad F_p \tag{5}$$

subject to

$$\begin{aligned} 0 &= f_C(x, u_C) \\ y_C^{LL} &\le y_C \le y_C^{UL} \\ u_C^{LL} &\le u_C \le u_C^{UL}, \end{aligned} \tag{6}$$

where $(\cdot)^{LL}$ and $(\cdot)^{UL}$ are the lower limits and upper limits respectively; F_p is the production rate that is defined as the effluent of the product tank minus the wash liquid.

Prospective active constraints are found to be the lower limits of the jacket temperatures of the 1st stage crystallizers, the upper limits for the temperature differences and slurry concentrations of the second stage crystallizers, and the slurry concentration in the underflow of the cyclone on the recycle stream. It has been found that around 2% increase in the production rate could be possible compared with the conventional operation.

Load distribution Load for the crystallizer is expressed as the temperature difference (ΔT) between the crystallizer and the jacket. For a prescribed production rate $\bar{F}_p$, flexible operation by distributing the loads between the two crystallizers at the second stage would be advantageous; when fouling of the crystallizer wall of one of the crystallizers is severe, which situation may be observed by decrease in the heat transfer coefficient, the load for that crystallizer is lowered while the load for the other crystallizer is increased to keep the production rate. For such cases, the following optimization problem can be conceived:

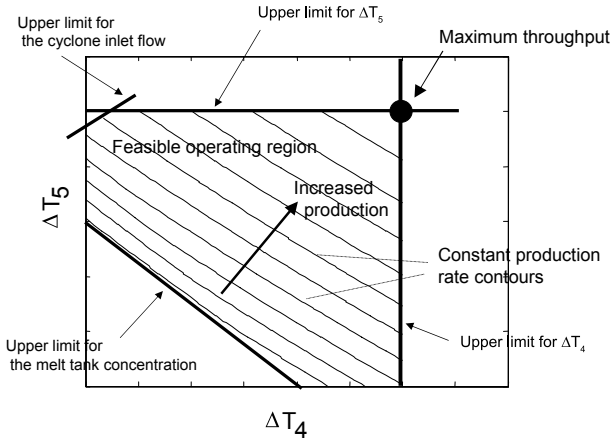

Fig. 5. Optimization landscape described as a contour plot of production rate

$$\min_{u_C} \quad w\Delta T_4 + (1-w)\Delta T_5 \tag{7}$$

subject to

$$\begin{aligned} 0 &= f_C(x, u_C) \\ F_p &= \bar{F}_p \\ y_C^{LL} &\le y_C \le y_C^{UL} \\ u_C^{LL} &\le u_C \le u_C^{UL}, \end{aligned} \tag{8}$$

where w ($0 \le w \le 1$) is the weight used for distributing the load.

Figure 5 shows the optimization landscape obtained by solving the minimization problem (7) for various values of production rate $\bar{F}_p$ and weight w, in which the load distribution for a fixed production rate is described as a contour plot in the $\Delta T_4 - \Delta T_5$ plane. The maximum throughput is realized when the upper limit constraints for both of the temperature differences become active, whereas the throughput is decreased for a moderate load where there is room for the temperature difference. The lower limits for the jacket temperatures of the 1st stage crystallizers and the upper limits for the slurry concentrations in the 2nd stage crystallizers and the underflow of the cyclone are always active.

4.3 Optimizing control

To realize the optimal operating policies derived in the previous subsection, a 6×6 multi-loop control is configured. As the manipulated and controlled variables, the following variables are selected:

Manipulated: T_4, T_5, α_7, α_9, F_w, F_{rec}
Controlled: Cs_4, ΔT_4, Cs_5, ΔT_5, Cs_9, x_{prod},

where Cs_4, Cs_5 and Cs_9 are the slurry concentrations of the 2nd stage crystallizers and the underflow of the cyclone separator on the recycle stream, x_{prod} is the para-xylene concentration in the product stream.

Constant setpoints are given to Cs_4, Cs_5, Cs_9, and x_{prod}, because constraints for these variables are known to be always active with the optimal operations, while the setpoints to ΔT_4 and ΔT_5 are varied according to the load distribution policy. Care should be taken in giving setpoints to ΔT_4 and ΔT_5, because other constraints for

Table 1. RGA analysis for the multi-loop controller design

	T_4	T_5	α_7	α_9	F_w	F_{rec}
Cs_4	0.0093	0.33	0.81	-0.19	0.041	0
ΔT_4	0.85	-0.33	0.18	-0.093	0.39	0
Cs_5	-0.057	0.055	0	0.0028	0	1.0
ΔT_5	-0.30	0.73	-0.0024	0.57	0.0074	-0.0027
Cs_9	-0.0034	0.33	0.0031	0.67	0.0022	0.0019
x_{prod}	0.5	-0.12	0.01	0.038	0.56	0.0

such variables as the cyclone inlet flow rate and melt tank concentration may become active.

A pairing of these variables in the multi-loop control system is determined through the relative gain array (RGA) analysis [Bristol (1966)] shown in Table 1.

5. SIMULATION STUDY

Figure 6 shows a simulation result of the designed control system when the setpoints of the temperature differences ΔT_4 and ΔT_5 are changed (all the numerical values are eliminated from the plot to keep any proprietary information confidential). For the first half of the simulation, the temperature difference ΔT_5 is changed stepwise, while the temperature difference of the other crystallizer ΔT_4 is held constant. This operation increases the production rate. For the second half, ΔT_4 is decreased stepwise while ΔT_5 is held constant. As a result, the load of the crystallizer 4 is reduced while the load of the crystallizer 5 is increased, compared with the initial state of the simulation.

Toward the end of the simulation when the load on the crystallizer 4 is reduced, the cyclone inlet flow almost hits the upper limit, which is anticipated from the analysis shown in Fig. 5.

6. CONCLUSION

A process model of an industrial crystallizer train for para-xylene recovery has been developed and a multi-loop control system has been configured.

Since the process is highly interactive due to the existence of the recycle streams, and the active constraints are subject to change depending upon operating conditions as shown in Fig. 5, application of multivariable model predictive control with constraint handling capability may be justified, if override control logic is regarded tedious.

One of the major concerns in the crystallizer operations is fouling of the crystallizer wall due to large supersaturation, which leads to decreased heat transfer and production rate. A monitoring and control system which is capable of identifying the deteriorating heat transfer coefficient to automatically adjust ΔT would be helpful.

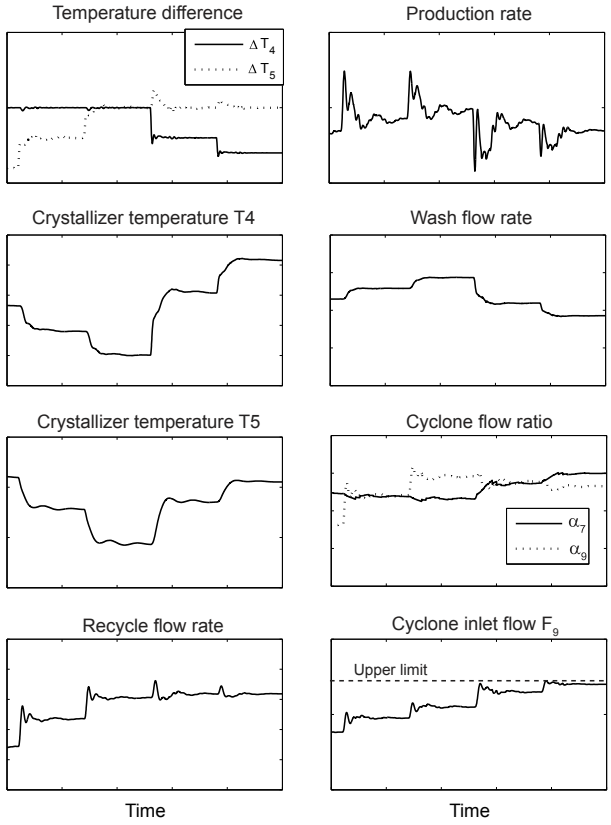

Fig. 6. Simulation result

REFERENCES

E.H. Bristol. On a new measure of interactions for multivariable process control. *IEEE Trans.*, volume AC-11, pages 133-134, 1966.

W.C. Chang and K.M. Ng. Synthesis of processing system around a crystallizer. *AIChE Journal*, volume 44, pages 2240–2251, 1998.

J. Garside. Industrial crystallization from solution. *Chem. Eng. Sci.*, volume 40, pages 3–26, 1985.

S. Hasebe, T. Hamamura, K. Naito, K. Sotowa, M. Kano, I. Hashimoto, H. Betsuyaku, and H. Takeda. Optimal operation of a continuous DTB crystallizer. *J. Process Control*, volume 10, pages 441–448, 2000.

C.H. Liu, D.H. Zhang, C.G. Sun, and Z.Q. Shen. The modelling and simulation of a multistage crystallizer. *The Chemical Engineering Journal*, volume 46, pages 9–14, 1991.

R. McGraw, S. Nemesure, and S.E. Schwartz. Properties and evolution of aerosols with size distributions having identical moments. *J. Aerosol Sci.*, volume 29, pages 761-772, 1998.

C.A. Mendez, J. Myers, S. Roberts, J. Logsdon, A. Vaia, and I.E. Grossmann. MINLP model for synthesis of paraxylene separation processess based on crystallization technology. *Proc. ESCAPE 15*, pages 829–834, Barcelona, Spain, 2005.

D.B. Patience, J.B. Rawlings, and H.A. Mohameed. Crystallization of para-xylene in scraped-surface crystallizers. *AIChE Journal*, volume 47, pages 2441–2451, 2001.

J.B. Rawlings, S.M. Miller, and W.R. Witkowski. Model identification and control of solution crystallization processes: a review. *Ind. Eng. Chem. Res.*, volume 32, pages 1275–1296, 1993.

J.D. Ward, C.C. Yu, and M.F. Doherty. Plantwide operation of processes with crystallization. *AIChE Journal*, volume 53, pages 2885–2896, 2007.

C. Wibowo, W.C. Chang, and K.M. Ng. Design of integrated crystallization systems. *AIChE Journal*, volume 47, pages 2474–2492, 2001.